

## Magnetic and magnetoelastic properties of $\text{PrNi}_5$ single crystal

V. M. T. S. Barthem,\* D. Gignoux, A. Naït-Saada, and D. Schmitt

*Laboratoire Louis Néel, Centre National de la Recherche Scientifique, 166X, 38042 Grenoble Cédex, France*

G. Creuzet

*Laboratoire de Physique des Solides, Bâtiment 510, Université Paris-Sud, 91405 Orsay, France*

(Received 29 June 1987)

An extensive experimental study by magnetic-resistivity, magnetostriction, and thermal-expansion measurements on a single crystal of the hexagonal  $\text{PrNi}_5$  compound is presented. The magnetoelastic results are quite satisfactorily interpreted within a model involving the crystal-field and quadrupolar interactions acting on the Pr ions and taking into account the Ni contribution. All the unusual features, especially the maxima observed around 15 K in the thermal variations of these properties, arise from crystal-field effects which lead to a nonmagnetic singlet ground state lying about 40 K below the first magnetic level. The induced Ni magnetism, although very small, strongly influences the observed behavior, especially the high-temperature magnetic susceptibility. The magnetoelastic coefficients  $B^{a1}$  and  $B^{a2}$  and the total quadrupolar coefficients  $G^a$  and  $G^e$  were determined, leading to the experimental evidence of antiferroquadrupolar interactions between rare-earth ions in  $\text{PrNi}_5$ .

### I. INTRODUCTION

The rare-earth compounds are of great interest for the study of magnetism. Indeed, because of the localization of the  $4f$  shell, it is possible to analyze quantitatively many physical measurements, leading to a determination of the different contributions to the Hamiltonian acting on the rare earth. However, due to the strongly anisotropic character of the properties, it is necessary to use a single crystal to properly determine the different interactions. Such an approach was successfully used in concentrated<sup>1,2</sup> and diluted<sup>3,4</sup> cubic rare-earth compounds. The best examples are the CsCl-type<sup>1</sup> or NaCl-type<sup>2</sup>  $RM$  compounds ( $R$ =rare earth,  $M=3d$ ,  $4d$ , or  $5d$  transition metal) where magnetoelastic and quadrupolar pair interactions were determined with very good accuracy.

In this context, hexagonal compounds are especially interesting to study, although the number of parameters required to describe the Hamiltonian is greater than that for cubic compounds. Indeed, they are the simplest systems with uniaxial anisotropy. Crystalline electric field (CEF) effects have been already investigated in hexagonal systems such as some  $R\text{Ni}_5$  compounds<sup>5-7</sup> and yttrium and scandium-based rare-earth alloys.<sup>8</sup> More recently, the single-ion magnetoelastic coupling was determined in these diluted alloys<sup>9,10</sup> as well as in Pr metal.<sup>11</sup> The concentrated  $R\text{Ni}_5$  compounds with a hexagonal structure provide a good opportunity to study the bilinear and quadrupolar interactions between rare-earth ions as well.

As a result of the outstanding permanent magnet properties of  $\text{SmCo}_5$ , the systematic studies of the properties of  $R\text{Co}_5$  and  $R\text{Ni}_5$  intermetallic compounds began nearly 20 years ago. In  $R\text{Co}_5$ , the Co is magnetic, and it

is very difficult to obtain a good determination of both  $R$  and Co contributions to the magnetic properties, especially the anisotropy due to the rare earth. In contrast, in  $R\text{Ni}_5$ , the  $3d$  shell of the Ni ions is almost filled up by the valence electron of the rare earth and its contribution to magnetism is very small, which leads to the possibility of studying rare-earth properties in isolation. Moreover, it is possible to obtain large single crystals of excellent quality.

Among the  $R\text{Ni}_5$  series,  $\text{PrNi}_5$  is a fascinating compound because, although small exchange interactions between Pr ions are present, it does not order down to a very low temperature because of the existence of a CEF singlet ground state as shown by magnetic susceptibility and heat capacity measurements.<sup>12</sup> Moreover, due to the large Van Vleck susceptibility corresponding to the relatively small separations of the single ground state from the higher excited states, this compound was successfully used for cooling through the adiabatic demagnetization process.<sup>13</sup> CEF and bilinear exchange parameters were previously determined from susceptibility measurements neglecting the Ni contribution.<sup>14</sup> These CEF parameters are close to those determined, almost at the same time, by inelastic neutron scattering.<sup>15</sup> Finally, low-temperature thermal-expansion measurements were analyzed taking into account the CEF effects.<sup>16,17</sup>

In this paper we present a systematic study of magnetic and magnetoelastic properties of  $\text{PrNi}_5$  single crystals. The first part (Sec. II) is devoted to the theoretical background used for the analysis of the experimental results. Section III concerns the susceptibility, magnetization, and resistivity measurements as well as their interpretation. Section IV describes the elastic and magnetoelastic measurements and their analysis. Finally, Sec. V is devoted to the discussion of all the results.

## II. THEORETICAL BACKGROUND

### A. The Hamiltonian

The relevant Hamiltonian describing the magnetic and magnetoelastic properties of the  $4f$  shell in a hexagonal symmetry may be written, using the operator-equivalent method<sup>18</sup> and the molecular field approximation, as

$$\mathcal{H} = \mathcal{H}_{\text{CEF}} + \mathcal{H}_D + \mathcal{H}_Q + \mathcal{H}_{\text{me}} + E_{\text{el}}. \quad (1)$$

In this expression,

$$\mathcal{H}_{\text{CEF}} = B_2^0 O_2^0 + B_4^0 O_4^0 + B_6^0 O_6^0 + B_6^6 O_6^6 \quad (2)$$

is the crystalline electric field (CEF) Hamiltonian, where the  $O_1^m$ 's are the Stevens equivalent operators.<sup>19</sup> The  $B_1^m$ 's are the CEF parameters. The equation

$$\mathcal{H}_D = -g_J \mu_B (\mathbf{H}_{\text{eff}} + n g_J \mu_B \langle \mathbf{J} \rangle) \cdot \mathbf{J} \quad (3)$$

includes the Zeeman coupling and the Heisenberg exchange interactions. In this expression,  $H_{\text{eff}}$  is the effective magnetic field acting on the rare-earth ion and  $n$  is the total isotropic bilinear exchange parameter, both terms taking into account the effect of the Ni magnetism (see Sec. II D). The two-ion quadrupolar Hamiltonian,

$$\begin{aligned} \mathcal{H}_Q = & -K^\alpha \langle O_2^0 \rangle O_2^0 - K^\epsilon (\langle O_2^2 \rangle O_2^2 + 4 \langle P_{xy} \rangle P_{xy}) \\ & - K^\zeta (\langle P_{zx} \rangle P_{zx} + \langle P_{yz} \rangle P_{yz}), \end{aligned} \quad (4)$$

which depends on three quadrupolar pair-interaction coefficients associated with the  $\Gamma_1$ ,  $\Gamma_5$ , and  $\Gamma_6$  representations, respectively, in the case of an hexagonal symmetry involves the following five second-order Stevens operators:

$$\begin{aligned} O_2^0 &= 3J_z^2 - J(J+1), \quad O_2^2 = J_x^2 - J_y^2, \\ P_{ij} &= \frac{1}{2}(J_i J_j + J_j J_i) \quad (ij = xy, yz, zx). \end{aligned}$$

This type of coupling has been extensively studied in cubic CsCl-type rare-earth intermetallic compounds<sup>20</sup> where it is responsible for the quadrupolar ordering observed in TmZn for example.<sup>21</sup> The one-ion magnetoelastic coupling,

$$\begin{aligned} \mathcal{H}_{\text{me}} = & -\frac{1}{\sqrt{6}} (B^{\alpha 1} \epsilon^{\alpha 1} + B^{\alpha 2} \epsilon^{\alpha 2}) O_2^0 \\ & -\frac{1}{\sqrt{2}} B^\epsilon (\epsilon_1^\epsilon O_2^2 + 2\epsilon_2^\epsilon P_{xy}) \\ & -\sqrt{2} B^\zeta (\epsilon_1^\zeta P_{zx} + \epsilon_2^\zeta P_{yz}), \end{aligned} \quad (5)$$

linear in strain, is limited to second-rank terms and written in symmetrized notation.<sup>22</sup> In this expression, the  $B^\mu$ 's are the four magnetoelastic coefficients associated with the corresponding normal strain modes in hexagonal symmetry,

$$\begin{aligned} \epsilon^{\alpha 1} &= \frac{1}{\sqrt{3}} (\epsilon_{xx} + \epsilon_{yy} + \epsilon_{zz}) \quad \text{for } \Gamma_1, \\ \epsilon^{\alpha 2} &= \frac{2}{3} \left[ \epsilon_{zz} - \frac{\epsilon_{xx} + \epsilon_{yy}}{2} \right] \quad \text{for } \Gamma_1, \\ \epsilon_1^\epsilon &= \frac{1}{\sqrt{2}} (\epsilon_{xx} - \epsilon_{yy}), \quad \epsilon_2^\epsilon = \sqrt{2} \epsilon_{xy} \quad \text{for } \Gamma_5, \\ \epsilon_1^\zeta &= \sqrt{2} \epsilon_{zx}, \quad \epsilon_2^\zeta = \sqrt{2} \epsilon_{yz} \quad \text{for } \Gamma_6. \end{aligned} \quad (6)$$

Within the harmonic hypothesis, the elastic energy is written as

$$\begin{aligned} E_{\text{el}} = & \frac{1}{2} c_{11}^\alpha (\epsilon^{\alpha 1})^2 + c_{12}^\alpha \epsilon^{\alpha 1} \epsilon^{\alpha 2} + \frac{1}{2} c_{22}^\alpha (\epsilon^{\alpha 2})^2 \\ & + \frac{1}{2} c^\epsilon [(\epsilon_1^\epsilon)^2 + (\epsilon_2^\epsilon)^2] + \frac{1}{2} c^\zeta [(\epsilon_1^\zeta)^2 + (\epsilon_2^\zeta)^2], \end{aligned} \quad (7)$$

where the  $c^\mu$ 's are the symmetrized background elastic constants without magnetic interactions.<sup>23</sup>

Minimizing the free energy with respect to the strains leads to the following equilibrium values for the normal strain modes  $\epsilon^\mu$ 's:

$$\begin{aligned} \epsilon^{\alpha 1} &= \frac{1}{\sqrt{6}} \frac{B^{\alpha 1} c_{22}^\alpha - B^{\alpha 2} c_{12}^\alpha}{c_{11}^\alpha c_{22}^\alpha - (c_{12}^\alpha)^2} \langle O_2^0 \rangle = A^{\alpha 1} \langle O_2^0 \rangle \quad \text{for } \Gamma_1, \\ \epsilon^{\alpha 2} &= \frac{1}{\sqrt{6}} \frac{B^{\alpha 2} c_{11}^\alpha - B^{\alpha 1} c_{12}^\alpha}{c_{11}^\alpha c_{22}^\alpha - (c_{12}^\alpha)^2} \langle O_2^0 \rangle = A^{\alpha 2} \langle O_2^0 \rangle \quad \text{for } \Gamma_1, \\ \epsilon_1^\epsilon &= \frac{1}{\sqrt{2}} \frac{B^\epsilon}{c^\epsilon} \langle O_2^2 \rangle = A^\epsilon \langle O_2^2 \rangle, \quad \epsilon_2^\epsilon = \sqrt{2} \frac{B^\epsilon}{c^\epsilon} \langle P_{xy} \rangle \quad \text{for } \Gamma_5, \\ \epsilon_1^\zeta &= \sqrt{2} \frac{B^\zeta}{c^\zeta} \langle P_{zx} \rangle, \quad \epsilon_2^\zeta = \sqrt{2} \frac{B^\zeta}{c^\zeta} \langle P_{yz} \rangle \quad \text{for } \Gamma_6. \end{aligned} \quad (8)$$

After replacing these  $\epsilon^\mu$ 's values in Eq. (5),  $\mathcal{H}_{\text{me}}$  appears to be indistinguishable from  $\mathcal{H}_Q$  [Eq. (4)] and both terms can be gathered into the total quadrupolar Hamiltonian

$$\begin{aligned} \mathcal{H}_{QT} = & -G^\alpha \langle O_2^0 \rangle O_2^0 - G^\epsilon (\langle O_2^2 \rangle O_2^2 + 4 \langle P_{xy} \rangle P_{xy}) \\ & - G^\zeta [\langle P_{zx} \rangle P_{zx} + \langle P_{yz} \rangle P_{yz}]. \end{aligned} \quad (9)$$

The total quadrupolar coefficients  $G^\mu$  then receive contributions from both the one-ion magnetoelastic and the quadrupolar pair interactions,

$$\begin{aligned} G^\alpha &= \frac{1}{6} \frac{(B^{\alpha 1})^2 c_{22}^\alpha - 2B^{\alpha 1} B^{\alpha 2} c_{12}^\alpha + (B^{\alpha 2})^2 c_{11}^\alpha}{c_{11}^\alpha c_{22}^\alpha - (c_{12}^\alpha)^2} + K^\alpha \\ &= G_{\text{me}}^\alpha + K^\alpha \quad \text{for } \Gamma_1, \\ G^\epsilon &= \frac{1}{2} \frac{(B^\epsilon)^2}{c^\epsilon} + K^\epsilon = G_{\text{me}}^\epsilon + K^\epsilon \quad \text{for } \Gamma_5, \\ G^\zeta &= \frac{2(B^\zeta)^2}{c^\zeta} + K^\zeta = G_{\text{me}}^\zeta + K^\zeta \quad \text{for } \Gamma_6. \end{aligned} \quad (10)$$

It is worth noting that the average value  $\langle O_2^0 \rangle$  is generally different from zero in hexagonal symmetry. As a consequence, the  $\Gamma_1$  term in  $\mathcal{H}_{QT}$  gives an additional contribution to the second-order CEF term in Eq. (2) as soon as  $B^{\alpha 1}$ ,  $B^{\alpha 2}$ , or  $K^\alpha$  are present.

In addition, this contribution is temperature dependent through the variation of  $\langle O_2^0 \rangle$ . Therefore, in case of strong quadrupolar coupling, it is worth taking into account explicitly this contribution in addition to the pure CEF one. On the other hand, from Eq. (8), there is simultaneously a quadrupolar contribution to the volume and to the ratio  $c/a$  of the hexagonal unit cell, even without a magnetic field. Applying a magnetic field modifies  $\langle O_2^0 \rangle$ , and thus modifies  $\epsilon^{\alpha 1}$  and  $\epsilon^{\alpha 2}$ , and the same relations as Eq. (8) may be written between the corresponding increments  $\delta\epsilon^{\alpha 1}$ ,  $\delta\epsilon^{\alpha 2}$ , and  $\delta\langle O_2^0 \rangle$  (see Sec. III C).

### B. Perturbation theory

The Hamiltonian [Eq. (1)] may be used in two ways for describing the magnetic properties of the  $4f$  shell. First, a direct diagonalization of the full Hamiltonian may be performed, in particular, in the presence of a magnetic field, and all the average values of the  $J_i$ 's ( $i=x,y,z$ ) and  $O_2^0, O_2^2, P_{ij}$ 's ( $ij=xy,yz,zx$ ) operators can be deduced, whence the magnitude and position of the rare-earth magnetic moment  $\mathbf{M}_R = g_J \mu_B \langle \mathbf{J} \rangle$  and the values of the strains  $\epsilon^\mu$  [through Eq. (8)]. This is the usual way for describing the magnetization and the magnetostriction curves (see Secs. III and IV).

The second way of using this Hamiltonian is to apply a perturbation theory in the paramagnetic state and for a low magnetic field.<sup>23</sup> It is thus possible to analytically express the free energy up to second order in the  $\epsilon^\mu$ 's and to fourth-order in  $H_{\text{eff}}$ . This leads to the following expansions of the magnetization  $M_R$  and of the increments  $\delta\langle O_2^m \rangle$  of the quadrupolar operators:

$$M_R = \chi_M^{(1)} H_{\text{eff}} + \chi_M^{(3)} H_{\text{eff}}^3 + \dots, \quad (11)$$

$$\delta\langle O_2^m \rangle = \chi_{Q_m} H_{\text{eff}}^2 + \dots, \quad (m=0,2), \quad (12)$$

where

$$\chi_M^{(1)} = \frac{\chi_0}{1-n\chi_0}, \quad (13)$$

is the usual first-order paramagnetic susceptibility and

$$\delta\langle O_2^m \rangle = \langle O_2^m \rangle_H - \langle O_2^m \rangle_{H=0},$$

$$\chi_M^{(3)} = \frac{1}{(1-n\chi_0)^4} \left[ \chi_0^{(3)} + \frac{2G^\alpha (\chi_{20}^{(2)})^2}{1-G^\alpha \chi_0^2} + \frac{2G^\epsilon (\chi_{22}^{(2)})^2}{1-G^\epsilon \chi_2^2} \right], \quad (14)$$

is the third-order paramagnetic susceptibility which includes a pure crystal field  $\chi_0^{(3)}$  and quadrupolar (magnetoelastic plus two-ion) contributions. We have

$$\chi_{Q_0} = \frac{\chi_{20}^{(2)}}{(1-n\chi_0)^2(1-G^\alpha \chi_2^2)}, \quad (15)$$

$$\chi_{Q_2} = \frac{\chi_{22}^{(2)}}{(1-n\chi_0)^2(1-G^\epsilon \chi_2^2)} \quad (16)$$

which are the quadrupolar susceptibilities associated with  $O_2^0$  and  $O_2^2$  respectively, which are the only second-

order operators involved when the magnetic field is applied along the three main symmetry directions of the hexagonal unit cell. In these expressions,  $\chi_0, \chi_0^{(3)}, \chi_2^m$ , and  $\chi_{2m}^{(2)}$  ( $m=0,2$ ) are CEF susceptibilities which may be calculated from the zero-field CEF level scheme, but the value of which depends on the direction of the magnetic field under consideration. For instance,  $\chi_{22}^{(2)}$  vanishes for a magnetic field applied along the  $c$  axis, where  $\langle O_2^0 \rangle$  is modified, but  $\langle O_2^2 \rangle$  remains zero. In the same way,  $\chi_0$  is anisotropic and changes according to whether the field is applied parallel or perpendicular to the  $c$  axis.<sup>24</sup>  $\chi_M^{(3)}$  and the  $\chi_{Q_m}$ 's explicitly depend on the quadrupolar coefficients  $G^\alpha$  and  $G^\epsilon$ . From the experimental measurement of these susceptibilities it is thus possible to determine these coefficients.

This perturbation theory has been widely applied to the rare-earth compounds in cubic symmetry,<sup>25,26</sup> and the complex expressions for the various CEF susceptibilities have been extended to the case of hexagonal and tetragonal symmetries in Ref. 23.

### C. Parastriction

In a general way, the relative change of length  $\lambda$  of a sample can be expressed as a function of the normal strain modes as<sup>22</sup>

$$\lambda = \frac{\delta l}{l} = \frac{1}{\sqrt{3}} \delta\epsilon^{\alpha 1} + \frac{1}{\sqrt{6}} \delta\epsilon^{\alpha 2} (3\beta_z^2 - 1) + \frac{1}{\sqrt{2}} \epsilon_1^\epsilon (\beta_x^2 - \beta_y^2) + \sqrt{2} \epsilon_2^\epsilon \beta_x \beta_y + \sqrt{2} \epsilon_3^\epsilon \beta_x \beta_z + \sqrt{2} \epsilon_4^\epsilon \beta_y \beta_z, \quad (17)$$

where the  $\beta_i$ 's are the direction cosines of the measurement direction. Restricting ourselves to measurements along the three main crystallographic directions  $\mathbf{a}, \mathbf{b}, \mathbf{c}$  of the orthohexagonal unit cell, the three normal strain modes  $\delta\epsilon^{\alpha 1}$ ,  $\delta\epsilon^{\alpha 2}$ , and  $\epsilon_1^\epsilon$  can be extracted through the following relevant combinations:

$$\begin{aligned} \frac{\delta V}{V} &= \frac{\delta a}{a} + \frac{\delta b}{b} + \frac{\delta c}{c} = \sqrt{3} \delta\epsilon^{\alpha 1}, \\ 2 \frac{\delta c}{c} - \frac{\delta a}{a} - \frac{\delta b}{b} &= \sqrt{6} \delta\epsilon^{\alpha 2}, \\ \frac{\delta a}{a} - \frac{\delta b}{b} &= \sqrt{2} \epsilon_1^\epsilon. \end{aligned} \quad (18)$$

In the paramagnetic phase and within the conditions of validity of the perturbation theory, Eqs. (8), (12), (15), (16), and (18) connect the various measured changes of length to the different susceptibilities involved according to the direction of the magnetic field. The magnetoelastic coefficients  $B^{\alpha 1}$ ,  $B^{\alpha 2}$ , and  $B^\epsilon$  and possibly the quadrupolar parameters  $G^\alpha$  and  $G^\epsilon$  can therefore be determined (the bilinear exchange parameter  $n$  being considered as known from magnetic susceptibility measurements). This type of parastriction measurements has been successfully performed in cubic systems such as rare-earth zinc compounds.<sup>25</sup>

We note that the investigation of the  $\zeta$  mode, i.e., the coefficients  $B^\zeta$ ,  $K^\zeta$ , and  $G^\zeta$ , is possible only by applying a magnetic field in a direction intermediate between the  $c$  axis and the base plane. On the other hand, in the

paramagnetic range it is possible to obtain information about the three modes  $\alpha 1$ ,  $\alpha 2$ , and  $\epsilon$ , by applying the magnetic field along the  $a$ ,  $b$ , and  $c$  directions only. In the case of a compound which orders magnetically, the results are more limited in the ordered phase where only the spontaneously magnetized state can be studied; that constitutes the main advantage of working in the nonordered phase.

#### D. Nickel contribution

As we will see below, the magnetic and magnetoelastic properties of  $\text{PrNi}_5$  mainly originate from the  $4f$ -Pr electrons. However, although Ni is nonmagnetic, its small contribution plays an important role especially at high temperature, i.e., when the  $4f$  contribution is small (see Sec. III and Fig. 1). Then contrary to the previous analysis of  $\text{PrNi}_5$  we take into account this Ni contribution within the itinerant electron model (Pauli paramagnet). The Ni magnetization can be then written as

$$\begin{aligned} \mathbf{M}_{\text{Ni}} &= \chi_{\text{Ni}}^0 (\mathbf{H}_i + n_{\text{NiNi}} \mathbf{M}_{\text{Ni}} + n_{\text{RNi}} \mathbf{M}_R) \\ &= \chi_{\text{Ni}} (\mathbf{H}_i + n_{\text{RNi}} \mathbf{M}_R) = \chi_{\text{Ni}} \mathbf{H}_i + \alpha \mathbf{M}_R, \end{aligned} \quad (19)$$

where  $\chi_{\text{Ni}}$  is the  $3d$  exchange enhanced susceptibility,

$$\chi_{\text{Ni}} = \frac{\chi_{\text{Ni}}^0}{1 - n_{\text{NiNi}} \chi_{\text{Ni}}^0}, \quad (20)$$

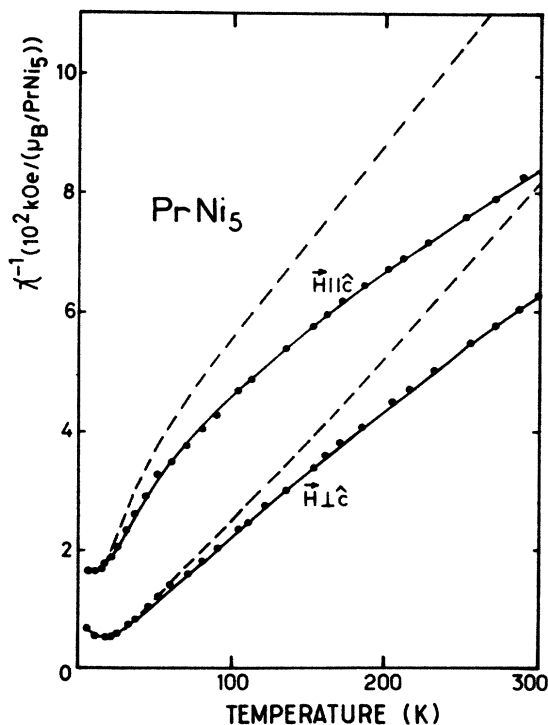


FIG. 1. Thermal variation of the reciprocal susceptibilities  $1/\chi_T$  of  $\text{PrNi}_5$  parallel and perpendicular to  $c$ . Black circles are the experimental values, solid lines are the calculated variations, and dashed lines are the variations corrected for the nickel contribution (see text).

$\mathbf{H}_i$  is the internal magnetic field (external field corrected for demagnetization effects),  $n_{\text{RNi}}$  is the molecular field coefficient between rare earth and nickel, and  $\alpha = \chi_{\text{Ni}} n_{\text{RNi}}$ .

The total magnetization can then be written as

$$\mathbf{M}_T = \mathbf{M}_R + \mathbf{M}_{\text{Ni}} = \chi_{\text{Ni}} \mathbf{H}_i + (1 + \alpha) \mathbf{M}_R. \quad (21)$$

The total field acting on a Pr ion includes the internal magnetic field and the contributions from both Pr-Pr and Pr-Ni exchange couplings,

$$\begin{aligned} \mathbf{H}_T &= \mathbf{H}_i + n_{\text{RR}} \mathbf{M}_R + n_{\text{RNi}} \mathbf{M}_{\text{Ni}} \\ &= \mathbf{H}_i (1 + \alpha) + n \mathbf{M}_R, \end{aligned} \quad (22)$$

where  $n = n_{\text{RR}} + \alpha n_{\text{RNi}}$  is the total isotropic bilinear exchange parameter acting on Pr ions. The Ni contribution therefore contributes by two ways to the rare earth: (i) By enhancing the applied magnetic field leading to an effective magnetic field  $\mathbf{H}_{\text{eff}} = \mathbf{H}_i (1 + \alpha)$ , and (ii) by enhancing the exchange interaction between Pr ions.

#### E. Perturbation theory with nickel

In the paramagnetic state, when the field is applied in one of the main symmetry directions,  $\mathbf{M}_R$ ,  $\mathbf{M}_{\text{Ni}}$ , and  $\mathbf{H}_{\text{eff}}$  are collinear and can then be written in a scalar form. Taking into account the Ni contribution, formula (11) of Sec. II B becomes

$$\begin{aligned} \mathbf{M}_R &= \chi_M^{(1)} \mathbf{H}_{\text{eff}} + \chi_M^{(3)} \mathbf{H}_{\text{eff}}^3 \\ &= \chi_M^{(1)} (1 + \alpha) \mathbf{H}_i + \chi_M^{(3)} (1 + \alpha)^3 \mathbf{H}_i^3, \end{aligned} \quad (23)$$

whence the expression for the total magnetization as a function of the internal field,

$$\mathbf{M}_T = [\chi_{\text{Ni}} + (1 + \alpha)^2 \chi_M^{(1)}] \mathbf{H}_i + (1 + \alpha)^4 \chi_M^{(3)} \mathbf{H}_i^3. \quad (24)$$

This leads to the following expressions for the total first- and third-order magnetic susceptibilities:

$$\chi_T^{(1)} = \chi_{\text{Ni}} + (1 + \alpha)^2 \chi_M^{(1)} \quad (25)$$

and

$$\chi_T^{(3)} = (1 + \alpha)^4 \chi_M^{(3)}. \quad (26)$$

We see that  $\chi_M^{(1)}$  is modified by  $\chi_{\text{Ni}}$  and  $\alpha$ , while  $\chi_M^{(3)}$  is modified by  $\alpha$  alone. In addition, the enhancement due to  $1 + \alpha$  is larger for  $\chi_M^{(3)}$  than for  $\chi_M^{(1)}$ .

### III. MAGNETIC PROPERTIES

Susceptibility and field dependence of magnetization were obtained from bulk magnetic measurements performed on a single crystal of spherical shape by using the extraction method in magnetic fields up to 80 kOe and in the temperature range 1.5–300 K. Measurements were extended up to 150 kOe below 4.2 K at the Service National des Champs Intenses in Grenoble.

#### A. Susceptibility

In Fig. 1 we have reported the thermal variation of the reciprocal susceptibilities measured parallel and per-

TABLE I. Crystal fields and exchange parameters obtained in PrNi<sub>5</sub> from different studies. We also show the parameters used to describe the Ni contribution to the magnetization.

Parameters	This work	Ref. 14	Ref. 15
$B_2^0$ (K)	$5.84 \pm 0.20$	5.82	5.57
$B_4^0$ ( $10^{-2}$ K)	$4.53 \pm 0.50$	4.49	4.20
$B_6^0$ ( $10^{-4}$ K)	$8.86 \pm 0.80$	8.77	9.40
$B_6^6$ ( $10^{-2}$ K)	$3.14 \pm 0.30$	3.10	3.02
$n$ (kOe/ $\mu_B$ )	$21 \pm 4$	28	
$10^2 \alpha$	$6.0 \pm 0.5$		
$\chi_{Ni}$ ( $10^{-4}$ e.m.u./mole)	$20.1 \pm 1.0$		

pendicular to the sixfold axis between 1.5 and 300 K. Because of the hexagonal symmetry, the susceptibility perpendicular to  $c$  is isotropic. On the contrary, a large magnetocrystalline anisotropy between the  $c$  axis and the basal plane is observed. In addition, at high temperature the variations of the reciprocal susceptibility are not linear and exhibit a negative curvature even at 300 K. Moreover, the effective moments deduced from the slopes of these variations at 300 K are much larger than the free Pr<sup>3+</sup> ion moment. This negative curvature as well as the weak values of the high-temperature slopes arise from the Ni contribution. Using Eq. (25), we were able to determine  $\chi_{Ni}$  and  $\alpha$  in order to deduce for  $\chi_M^{(1)} = \chi_0 / (1 - n\chi_0)$  a thermal dependence characteristic of the Pr contribution. The value obtained are given in Table I. The variations of  $1/\chi_M^{(1)}$  then obtained are re-

ported as dashed lines in Fig. 1, showing the large Ni effect at high temperatures.

At low temperature, as previously observed,<sup>14</sup> the susceptibility perpendicular to  $c$  passes through a large maximum around 16 K, whereas the variation decreases monotonically along the  $c$  axis (see Fig. 2). These results are quantitatively slightly different from those reported in Ref. 14 (see below). The large maximum arises from the competition between the Curie and the Van Vleck terms in a system with a nonmagnetic singlet ground state.<sup>14</sup>

Besides the Ni contribution determined above, the magnetic susceptibility depends explicitly on five parameters: the four CEF parameters through  $\chi_0$  and the total exchange coefficient  $n$ . As stated above, the quadrupolar parameter  $G^a$  intervenes only in an indirect way by contributing to the  $B_2^0$  parameter. We will see below that this contribution is negligible compared to that of the pure CEF  $B_2^0$  term.

The parameters previously reported<sup>14,15</sup> (see Table I) were determined without taking into account the nickel and thus cannot describe our results (dashed lines in Fig. 2). We were able to fit consistently the variations of Figs. 1 and 2, as well as the results previously reported (inelastic neutron scattering<sup>15</sup> and heat capacity<sup>12</sup>) by taking a slightly different set of parameters (see Table I). These parameters were then kept fixed in the following analysis.

## B. Resistivity

It is well known that there exists a close correlation between heat capacity and resistivity. Therefore, as a large Schottky anomaly is observed by heat capacity around 16 K (Ref. 12), one can expect large thermal effects on the resistivity in the same temperature range. We have measured the resistivities of polycrystalline samples of PrNi<sub>5</sub> and LaNi<sub>5</sub> between 1.5 and 300 K using an ac four-probe method. The thermal dependence of these resistivities between 1.5 and 50 K are shown in Fig. 3. The comparison between the two curves provides evidence for a large magnetic contribution on PrNi<sub>5</sub> above 4 K. The importance of this contribution is illustrated in the inset of Fig. 3 in which we have plotted the thermal variation of  $d\rho_m/dT$ , where  $\rho_m = \rho(\text{PrNi}_5) - \rho(\text{LaNi}_5)$  [ $\rho(\text{LaNi}_5)$  being considered as equal to the electronic and lattice contributions of PrNi<sub>5</sub> and  $\rho_m$  representing the magnetic part]. This variation

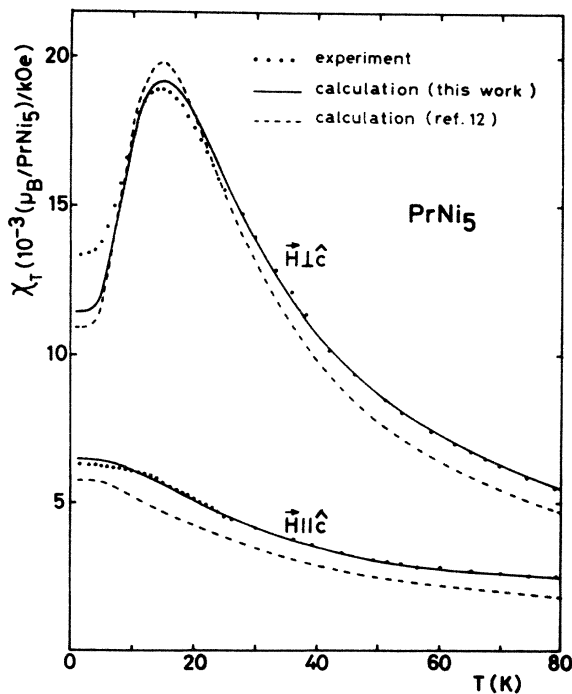


FIG. 2. Thermal variation of the low-temperature susceptibilities  $\chi_T$  of PrNi<sub>5</sub> parallel and perpendicular to  $c$ . Black circles are the experimental values. Solid and dashed lines are the variations calculated with our parameters and with those given in Ref. 12, respectively.

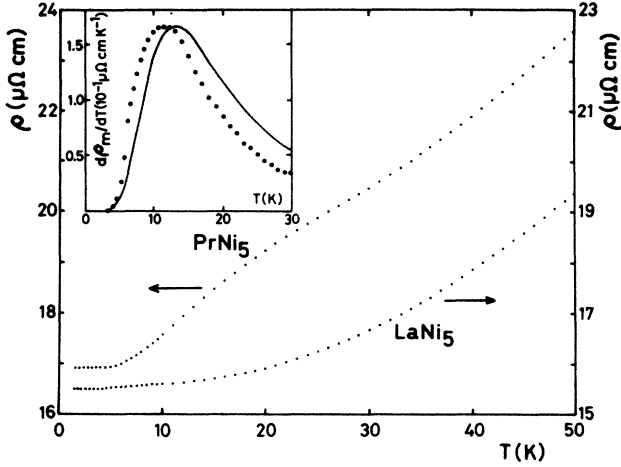


FIG. 3. Thermal dependences of resistivities of  $\text{PrNi}_5$  and  $\text{LaNi}_5$  between 1.5 and 50 K. The inset shows the thermal dependence of the thermal derivative  $d\rho_m/dT$  of the magnetic contribution  $\rho_m$  to the resistivity of  $\text{PrNi}_5$ . Black circles are the experimental values while solid line is the calculated variation.

is quite similar to that observed in the specific heat, especially it exhibits a large maximum in the same temperature range. This Schottky-like anomaly arises from the spin disorder (SD) resistivity  $\rho_{\text{SD}}$ , which, in this paramagnetic compound, is characteristic of the CEF splitting.<sup>28</sup> The  $\rho_{\text{SD}}$  resistivity was calculated with the above CEF parameters and the thermal variation of its thermal derivative is shown as a solid line in the inset of Fig. 3. In spite of a small shift, the calculated variation gives quite a good account of the experimental data.

### C. Field dependence of magnetization

The field dependences of magnetization measured up to 150 kOe at 1.5 K along the a, b, and c axes of the orthohexagonal cell are shown in Fig. 4. In agreement with the susceptibility measurements, the c axis is the hard magnetization direction. In the basal plane and in low field the magnetization measured along the a and b axes are identical, in agreement with the isotropy of the initial susceptibility (see Sec. III A). When the field is increased, an anisotropy between both axes appears leading to the b axis as the easy magnetization direction. This anisotropy arises from the effect of the  $B_6^6$  CEF term and/or that of the quadrupolar interactions (see below).

It is worth noting that along this axis a positive curvature more pronounced around 70 kOe is observed. Such a behavior, quite unusual for a paramagnetic compound, is more similar to a metamagnetic transition in an antiferromagnet. This transition has the same CEF origin as the maximum of the susceptibility observed perpendicular to c at 16 K (see Sec. III A). Note that the existence of a maximum of the thermal dependence of the susceptibility associated with a metamagnetic transition at low temperatures are also observed in other systems which

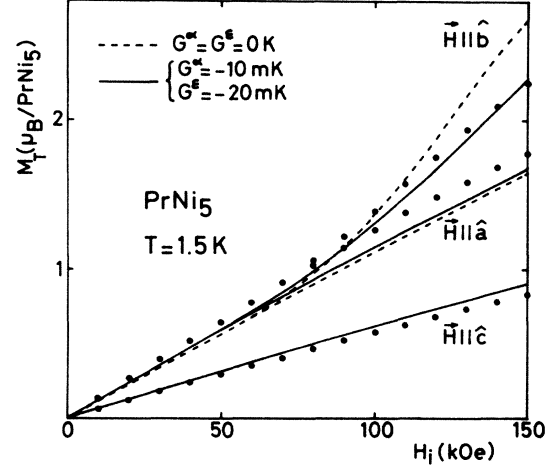


FIG. 4. Field dependence of magnetization at 1.5 K along the three main symmetry directions of  $\text{PrNi}_5$ . Black circles are the experimental values. Solid and dashed lines are the variations calculated with and without quadrupolar interactions, respectively.

do not order magnetically, such as the itinerant electron metamagnets.<sup>29</sup> This is characteristic of systems with a nonmagnetic ground state and magnetic excited states.

This behavior along b, as well as the variations along a and c, are qualitatively well accounted for by the calculated field dependences of magnetization using the Ni and Pr parameters determined above (see Fig. 4). The disagreement in high fields between the calculated and experimental variations can arise from other contributions than those considered, such as the quadrupolar coupling. This coupling, which does not appear explicitly in the first-order susceptibility, appears in the expression of the third-order term and then modifies the high-field magnetization.

As seen in Eq. (14), a clear way to demonstrate this quadrupolar contribution is to investigate  $\chi_M^{(3)}$ . The usual way to extract  $\chi_M^{(3)}$  is to plot the isothermal variations of the ratio  $M_T/H_i$  as a function of  $H_i^2$ . In low field, linear variations are expected; the value in zero field gives  $\chi_M^{(1)}$ , while the slope provides  $\chi_M^{(3)}$ . Such an analysis was successfully used to determine the quadrupolar interactions in cubic compounds.<sup>26</sup>

In Fig. 5 we show such isotherms for  $\text{PrNi}_5$  when the field is applied along b. These variations are not linear especially at low temperatures. This can arise from the enhancement, when temperature is decreased, of higher-order terms in field or from the presence of impurities such as magnetic  $\text{Pr}^{3+}$  ions. In order to get rid of this last contribution, which could explain the large increase of  $M_T/H_i$  at low temperature and in low field, we have analyzed only the variations in high field, especially their slopes  $\chi_{\text{HF}}^{(3)}$ . Such an analysis is justified by the calculation which shows, as illustrated in Fig. 5 for  $T=13$  K, that the  $H_i^2$  dependences of  $M_T/H_i$  are much better accounted for in high field than in low field.

In Fig. 6 we show the thermal variations below 30 K of the  $\chi_{\text{HF}}^{(3)}$ 's measured along the a, b, and c axes in a 65-

kOe internal field. A large anisotropy between the six-fold axis and the basal plane can be seen. Along *c*, as observed in many compounds,<sup>26</sup>  $\chi_{\text{HF}}^{(3)}$  is negative. However, its absolute value is weak and decreases roughly linearly as the temperature is increased. On the contrary, along *a* and *b*,  $\chi_{\text{HF}}^{(3)}$  is one order of magnitude larger and exhibits an unusual thermal dependence mainly characterized by a change of sign at 8 K. This must be related to the CEF levels of the Pr<sup>3+</sup> ions.

According to the nature of the CEF levels,  $\chi_{\text{HF}}^{(3)}$  is expected to either (i) vary as  $1/T^3$  at low temperature when the ground state is magnetic or (ii) to present a saturation at low temperature and/or a change of sign when the ground state is nonmagnetic (see Fig. 2 of Ref. 26). The behavior of  $\chi_{\text{HF}}^{(3)}$  in PrNi<sub>5</sub> is clearly characteristic of a CEF singlet ground-state system.

Using the parameters describing Ni and Pr determined above, we have calculated through the diagonalization of the Hamiltonian acting on Pr the thermal dependences of  $\chi_{\text{HF}}^{(3)}$  along the three symmetry directions and for a 65-kOe internal field (dashed lines in Fig. 6). Along *c* the agreement is satisfactory. In contrast, along *a* and *b*, although the shape of the variation is rather well accounted for (especially the change of sign), there remains a shift. Taking into account the quadrupolar coupling coefficients  $G^\alpha = -10$  mK and  $G^\epsilon = -20$  mK, the fit (variations in solid lines) is significantly improved.  $G^\epsilon$  has no effect along *c* and the role of  $G^\alpha$  is negligible along this direction. Note that the improvement is also noticeable on the magnetization in high field, mainly along the *b* axis (see Fig. 4). Another set of parameters such as  $G^\alpha = -30$  mK and  $G^\epsilon = 0$  mK would also give a

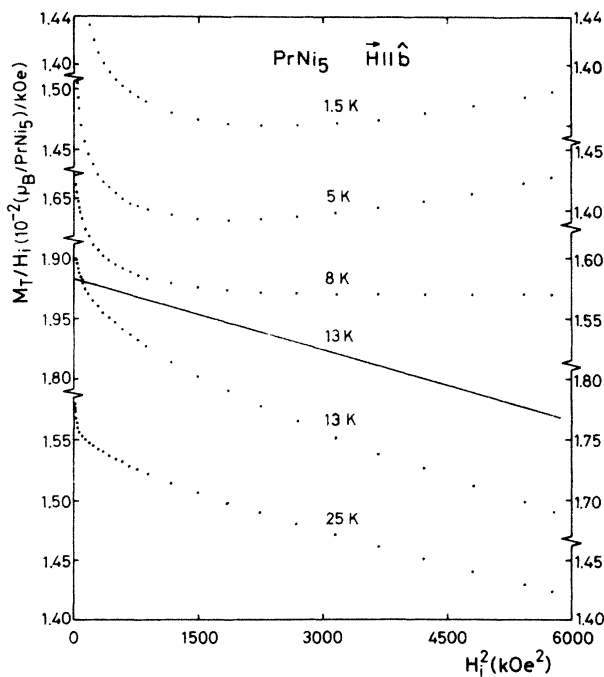


FIG. 5. PrNi<sub>5</sub>: variation of  $M_T/H_i$  vs  $H_i^2$  at different temperatures for the *b* axis.

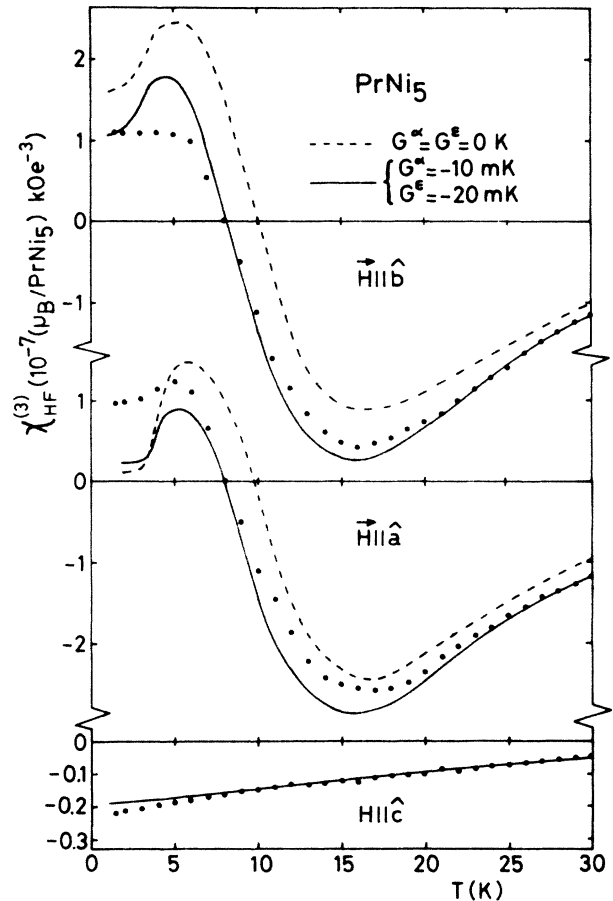


FIG. 6. PrNi<sub>5</sub>: thermal variation of the  $\chi_{\text{HF}}^{(3)}$  susceptibility below 30 K along the *a*, *b*, and *c* axes in a 65-kOe internal field (see text). Points are experimental values, solid lines are calculated with  $G^\alpha = -10$  mK and  $G^\epsilon = -20$  mK, and dashed lines are calculated without quadrupolar interactions. Both calculated variations are identical for the *c* axis.

rather good agreement; however, it would lead to a worse agreement for magnetoelastic properties (see below). These results are, to our knowledge, the first determination of quadrupolar interactions (magnetoelastic plus two ion) by magnetic measurements in a noncubic rare-earth compound.

#### IV. MAGNETOELASTIC PROPERTIES

The magnetoelastic measurements were performed on a cubic sample of about 4-mm sides obtained by spark cutting, with faces perpendicular to the *a*, *b*, and *c* axes, respectively. The magnetostriction and thermal-expansion measurements along these three axes were made successively by using a capacitance method with a relative sensitivity of about  $10^{-8}$  for  $\delta l/l$ . The dilatometer was built in copper and was calibrated with high-purity copper and aluminum specimens. The thermal expansion measurements were performed in the temperature range 1.2–75 K. The magnetostriction measurements were done in the temperature range 1.2–20 K.

The magnetic field could be applied parallel to the strain measurement direction ( $H$  up to 70 kOe) or rotated in the plane perpendicular to this direction ( $H$  up to 40 kOe).

### A. Magnetostriction

Whatever is the direction of measurements, the magnetostriction is at least one order of magnitude smaller when the field is applied along  $c$  than perpendicular to  $c$ . This is well illustrated in Fig. 7 for the magnetostriction measured along  $c$ . Within the experimental accuracy the magnetostrictions follow a  $H_i^2$  law. The thermal variations of the coefficient  $d(\delta c/c)/dH_i^2$  of this law are shown in the insets of Fig. 7. When the field is along  $c$  this thermal variation is meaningless because of large experimental error bars. These uncertainties do not arise from the inaccuracy of the measurement but from a slight disorientation of the sample with regard to the applied field. Indeed, when the field is applied close to a hard magnetization axis in systems with large anisotropy, such a disorientation leads to strong spurious contributions. In contrast, when the field is applied perpendicular to  $c$ , the thermal variation of this coefficient is unusual and exhibits a large maximum around 11 K. Such a maximum is also observed when the magnetostriction is measured along the  $a$  and  $b$  axes. Note that a previous study, performed on a polycrystal and below 50

kOe, surprisingly did not reveal any noticeable magnetostriction.<sup>16</sup>

In the following, we will consider the measurements performed when the field is applied along the  $b$  axis. From the measurements of length changes along the  $a$ ,  $b$ , and  $c$  axes we can deduce the symmetrized strains  $\delta\epsilon^{\alpha 1}, \delta\epsilon^{\alpha 2}, \epsilon_1^\epsilon$  [see Eq. (18)]. The values of  $\epsilon_1^\epsilon$  are meaningless because they result from the difference of values of  $\delta a/a$  and  $\delta b/b$  which are very close to each other. The  $\delta\epsilon^{\alpha 2}$  values are the largest because they result from the sum of contributions with the same sign, while the  $\delta\epsilon^{\alpha 1}$  values are smaller and thus less accurate because they result from contributions with opposite sign (see Fig. 8). As mentioned above for the magnetostriction along the  $c$  axis, at any temperature  $\delta\epsilon^{\alpha 1}$  and  $\delta\epsilon^{\alpha 2}$  follow a  $H_i^2$  law in a large range of magnetic fields (see Fig. 9). The thermal dependences of  $\sqrt{3}d(\delta\epsilon^{\alpha 1})/dH_i^2$  and  $\sqrt{6}d(\delta\epsilon^{\alpha 2})/dH_i^2$  are shown in Fig. 10. They exhibit around 11 K a large maximum similar to that observed on the thermal variation of the magnetic susceptibility in the basal plane.

According to Eqs. (8) and (12), the field dependences of  $\delta\epsilon^{\alpha 1}$  and  $\delta\epsilon^{\alpha 2}$  are directly related to the quadrupolar susceptibility  $\chi_{Q_0}$ . Using the CEF and bilinear exchange

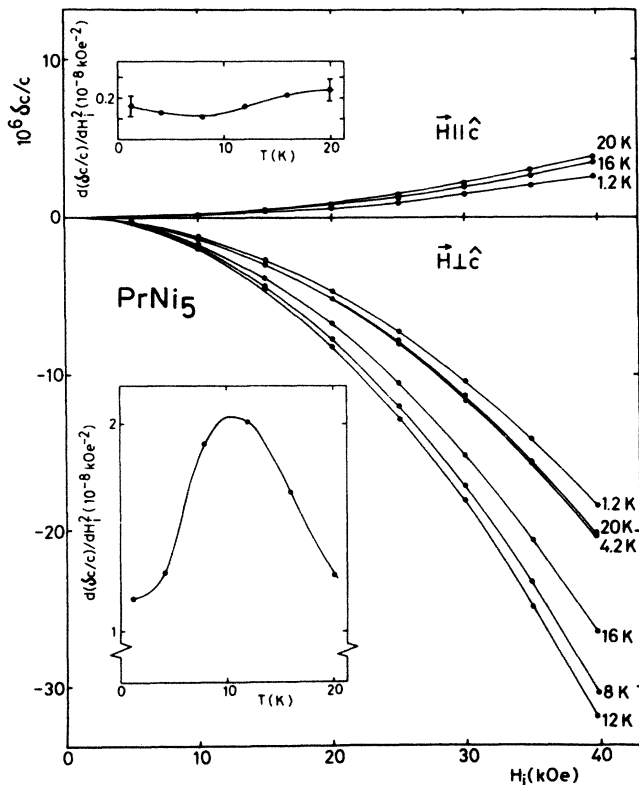


FIG. 7. Magnetostriction of  $\text{PrNi}_5$  measured along the  $c$  axis for fields parallel and perpendicular to  $c$ . The insets show the corresponding thermal dependences of  $d(\delta c/c)/dH_i^2$ .

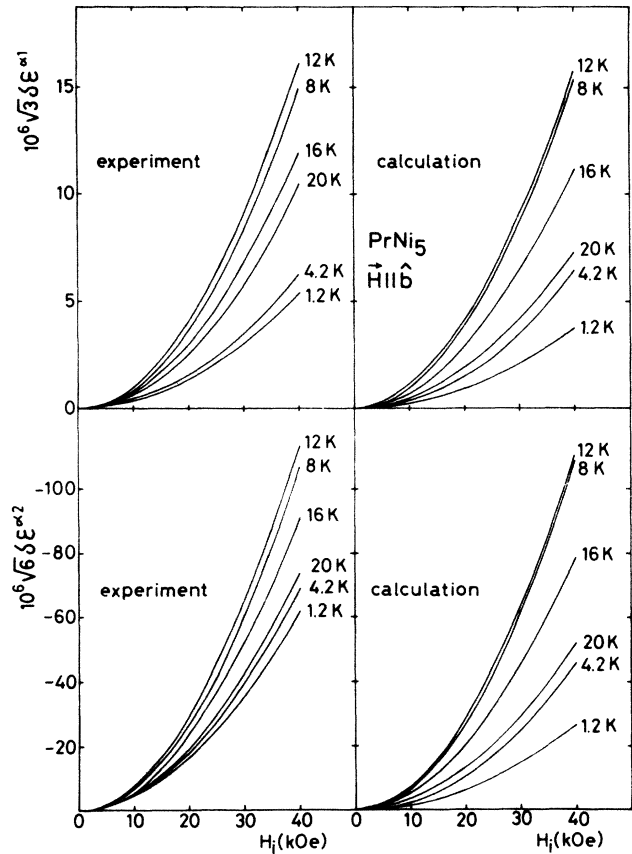


FIG. 8. Experimental and calculated field dependences of  $\sqrt{3}\delta\epsilon^{\alpha 1} = \delta V/V = (\delta a/a) + (\delta b/b) + (\delta c/c)$  and  $\sqrt{6}\delta\epsilon^{\alpha 2} = 2(\delta c/c) - (\delta a/a) - (\delta b/b)$  at different temperatures when the field is applied along  $b$ . Calculation was performed with  $G^a = -10$  mK and  $G^\epsilon = -20$  mK.

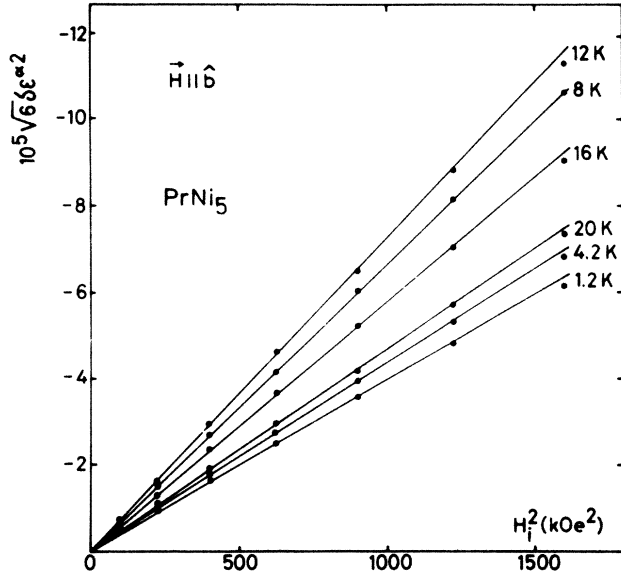


FIG. 9. Experimental variations of  $\sqrt{6}\delta\epsilon^{\alpha 2}=2(\delta c/c)-(\delta a/a)-(\delta b/b)$  vs  $H_i^2$  at different temperatures when the field is applied along the **b** axis.

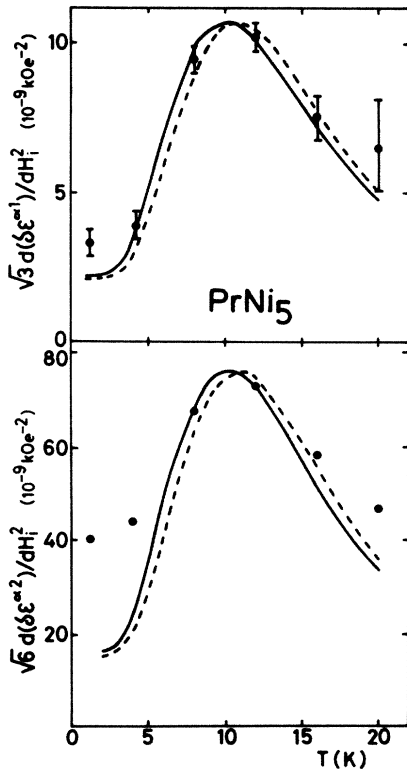


FIG. 10. Experimental and calculated thermal dependences of  $\sqrt{3}d(\delta\epsilon^{\alpha 1})/dH_i^2$  and  $\sqrt{6}d(\delta\epsilon^{\alpha 2})/dH_i^2$  when the field is applied along the **b** axis. Solid lines and dashed lines are the calculations with  $G^{\alpha}=-10$  mK and  $G^{\epsilon}=-20$  mK and  $G^{\alpha}=G^{\epsilon}=0$ , respectively.

parameters determined above, the thermal variation of  $\chi_{Q_0}$  calculated from Eq. (15) with  $G^{\alpha}=0$  has been normalized on the experimental values leading to  $A^{\alpha 1}=-1.44\times 10^{-5}$  and  $A^{\alpha 2}=7.23\times 10^{-5}$  (dashed line in Fig. 10). The agreement is quite satisfactory, especially with regard to the existence of the maximum around 11 K. As a second step we have used the value of  $G^{\alpha}$  determined above from the analysis of the magnetization curves. This leads to the calculated thermal dependences of  $d(\delta\epsilon^{\alpha 1})/dH_i^2$  and  $d(\delta\epsilon^{\alpha 2})/dH_i^2$  shown as solid lines in Fig. 10. The agreement with experimental variations is slightly better than with  $G^{\alpha}=0$ , especially for the curves corresponding to  $T=8$  K and 12 K, which are the experimental values obtained with the highest accuracy. The diagonalization of the full Hamiltonian using these parameters describes the field dependences of the magnetostriction well (Fig. 8).

The determination of the magnetoelastic coefficients  $B^{\alpha 1}$  and  $B^{\alpha 2}$  from  $A^{\alpha 1}$  and  $A^{\alpha 2}$  [Eq. (8)] necessitates the knowledge of the elastic constants  $c_{ij}^{\alpha}$ . These values were obtained from ultrasonic measurements<sup>30</sup> at 300 K and have led to  $c_{11}^{\alpha}=19.3\times 10^5$  K,  $c_{12}^{\alpha}=0.80\times 10^5$  K, and  $c_{22}^{\alpha}=9.6\times 10^5$  K. Using a thermal variation of the elastic constants analogous to that observed in CeNi<sub>5</sub>,<sup>31</sup> the values then obtained for the magnetoelastic coefficients are  $B^{\alpha 1}=-54$  K and  $B^{\alpha 2}=168$  K. Using these values in Eq. (10) leads to an estimate of the one-ion magnetoelastic contribution to the quadrupolar parameters:  $G_{me}^{\alpha}=5.3$  mK.

### B. Thermal expansion

We show in Fig. 11 the thermal expansions of PrNi<sub>5</sub> and LaNi<sub>5</sub> in the temperature range 1.2–40 K. In LaNi<sub>5</sub>, the thermal expansion is isotropic. In PrNi<sub>5</sub>, whereas the thermal expansion is isotropic in the basal plane, a large anisotropy is observed between the **c** axis and the basal plane. We have assumed that the thermal expansion of LaNi<sub>5</sub> corresponds to the electronic and lattice contributions of PrNi<sub>5</sub> and was subtracted from the raw data of the thermal expansion of PrNi<sub>5</sub> to deduce the magnetic contribution. In Fig. 12 we show the temperature dependences of the linear thermal expansion coefficients measured parallel and perpendicular to the hexagonal axis. These coefficients of opposite sign exhibit a large maximum around 13 K. Below 12 K, the variations are similar to those reported in Ref. 16 in spite of differences in magnitude along the **c** axis.

From the formulae (8) and (17) we obtain

$$\frac{\delta c}{c} = \frac{1}{\sqrt{3}} (\delta\epsilon^{\alpha 1} + \sqrt{2}\delta\epsilon^{\alpha 2}) = \left[ \frac{1}{\sqrt{3}} A^{\alpha 1} + \frac{2}{3} A^{\alpha 2} \right] \delta\langle O_2^0 \rangle, \quad (27)$$

$$\frac{\delta b}{b} = \sqrt{3} \left[ \delta\epsilon^{\alpha 1} - \frac{1}{\sqrt{2}}\delta\epsilon^{\alpha 2} - \frac{3}{2}\epsilon_1^{\epsilon} \right]$$

$$= \left[ \frac{1}{\sqrt{3}} A^{\alpha 1} - \frac{1}{\sqrt{6}} A^{\alpha 2} \right] \delta\langle O_2^0 \rangle - \frac{1}{\sqrt{2}} A^{\epsilon} \langle O_2^0 \rangle.$$

In the paramagnetic range and in the absence of any

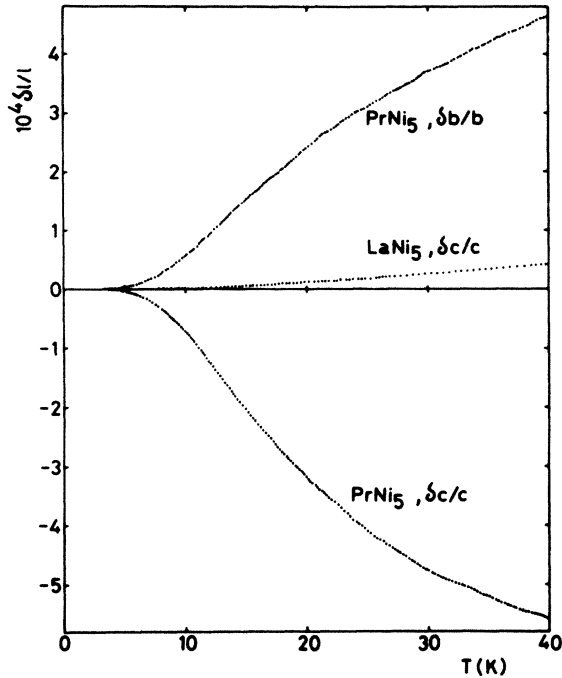


FIG. 11. Thermal expansion measured along the *b* and *c* axes for  $\text{PrNi}_5$  and  $\text{LaNi}_5$ , respectively. Note that in  $\text{LaNi}_5$ , thermal expansion is isotropic.

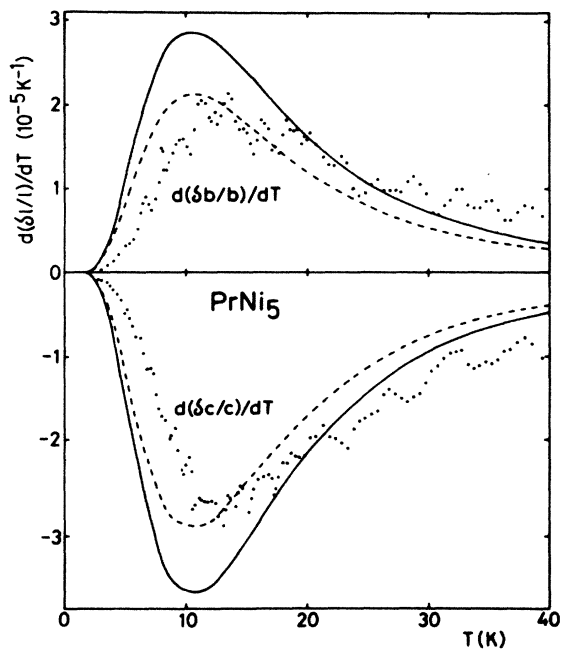


FIG. 12. Calculated and measured thermal variations of the linear thermal expansion coefficients along *b* and *c* axes in  $\text{PrNi}_5$ . The calculation was performed with  $G^\alpha = -10 \text{ mK}$  and  $G^\epsilon = -20 \text{ mK}$ . Solid lines correspond to  $B^{\alpha 1} = -54 \text{ K}$  and  $B^{\alpha 2} = 168 \text{ K}$ ; dashed lines correspond to  $B^{\alpha 1} = -35 \text{ K}$  and  $B^{\alpha 2} = 132 \text{ K}$ .

TABLE II. Magnetoelastic and quadrupolar parameters in  $\text{PrNi}_5$ .

$B^{\alpha 1}$	$-54 \pm 8 \text{ K}$
$B^{\alpha 2}$	$168 \pm 8 \text{ K}$
$B^\epsilon$	$< 22 \text{ K}$
$G_{me}^\alpha$	$5.3 \pm 0.8 \text{ K}$
$G^\alpha$	$-10 \pm 5 \text{ mK}$
$G_{me}^\epsilon$	$< 0.5 \text{ mK}$
$G^\epsilon$	$-20 \pm 10 \text{ mK}$

magnetic field  $\langle O_2^2 \rangle = 0$  and thus  $\delta b/b$  depends only on  $\langle O_2^0 \rangle$ . Thus the thermal dependences of  $\delta c/c$  and  $\delta b/b$  are proportional to that of  $\delta \langle O_2^0 \rangle$ . With  $G^\alpha = -10 \text{ mK}$  and  $G^\epsilon = -20 \text{ mK}$ , we have calculated the thermal dependences of the linear thermal expansion coefficients  $d(\delta c/c)/dT$  and  $d(\delta b/b)/dT$  (solid lines in Fig. 12). Although larger than the experimental points at low temperatures, these variations give a rather good account of the measurements. Normalizing the calculated variation on the maxima to the experimental ones would lead to slightly different magnetoelastic coefficients ( $B^{\alpha 1} = -34 \text{ K}$  and  $B^{\alpha 2} = 131 \text{ K}$ , dashed lines in Fig. 12).

## V. DISCUSSION

In this paper an extensive experimental study on the  $\text{PrNi}_5$  hexagonal compound is presented. All the measurements, i.e., magnetic susceptibility, field dependence of magnetization, resistivity, magnetostriction, and thermal expansion, were satisfactorily interpreted within the same set of parameters involved in the Hamiltonian acting on the Pr ions and taking into account the Ni contribution (see Tables I and II). All the unusual features of  $\text{PrNi}_5$ , especially the maxima observed in the vicinity of 15 K in the thermal dependences of these properties, are due to the spacing and the nature of the low-lying CEF levels.

The CEF and bilinear exchange parameters are quite consistent with those determined previously (Table I). The slight differences could originate from substitutions or off stoichiometric effects associated with the preparation of each sample.

In our analysis only the isotropic bilinear exchange interaction was considered. The existence of a weak anisotropic term was found in  $\text{GdNi}_5$  and led to a very small anisotropy of the observed magnetic susceptibility along and perpendicular to *c*.<sup>27</sup> Extrapolating this term to  $\text{PrNi}_5$ , according to the de Gennes law, leads to a quite negligible value.

Note that the value of the total exchange interaction *n* is undercritical in  $\text{PrNi}_5$ , preventing the appearance of any magnetic order. Such order would take place at  $T_{\text{max}} = 15 \text{ K}$  for a critical value  $n_c = 1/\chi_T^{(1)} = 52.6 \text{ kOe}/\mu_B$ . It is worth noting that, due to the particular shape of the susceptibility, for *n* values slightly larger than this critical value the magnetic order would take place only in a small range of temperatures around 15 K.

### A. Nickel contribution

So far in this discussion the Ni contribution has been neglected. In fact we have determined its magnitude and shown that, although small, it strongly influences the observed properties, especially the high-temperature magnetic susceptibility. The Ni susceptibility  $\chi_{\text{Ni}}$ , considered as temperature independent, is very close to that determined in the other RNi<sub>5</sub> compounds.<sup>6,7,32,33</sup>

As in the other RNi<sub>5</sub> compounds,<sup>6,7,33</sup> the sign of the molecular field coefficient  $n_{\text{RNi}}$  corresponds to a negative interaction between the spins of the rare-earth and those of the Ni atoms. This interaction is quite comparable to that determined in the other RNi<sub>5</sub> compounds as well.

### B. Magnetoelastic coefficients

Our study allowed us to determine the  $B^{\alpha 1}$  and  $B^{\alpha 2}$  magnetoelastic coefficients. The rather good agreement between the values of these coefficients determined by two techniques (magnetostriction and thermal expansion) shows that the volume and axial strain dependences of the exchange interactions,<sup>11</sup> if present, only contribute weakly to the magnetostriction. We have also estimated these magnetoelastic coefficients within the point-charge model. Considering only the eight first Pr<sup>3+</sup> nearest neighbors leads to values ( $B^{\alpha 1} = -48$  K and  $B^{\alpha 2} = +262$  K) of the same sign and of similar magnitude as the experimental values.

As shown above, the quadrupolar parameter  $G^{\alpha}$  contributes to the second-order CEF parameter  $B_2^0$  even

without magnetic field. Taking into account a calculated value  $\langle O_2^0 \rangle = 7$ , the determined value of  $G^{\alpha}$  contributes for about 1% to the  $B_2^0$  value. It thus appears quite justified to neglect such a contribution to the CEF in PrNi<sub>5</sub>.

### C. Two-ion quadrupolar interactions

The magnetoelastic contribution  $G_{\text{me}}^{\alpha}$  to  $G^{\alpha}$  and  $G_{\text{me}}^{\epsilon}$  to  $G^{\epsilon}$  being always positive, the negative values of  $G^{\alpha}$  and  $G^{\epsilon}$  lead to values of the two-ion quadrupolar interactions still more negative:  $K^{\alpha} \simeq -15$  mK and  $K^{\epsilon} \leq -20$  mK. This constitutes, to our knowledge, the first evidence for the existence of antiferroquadrupolar interactions between rare-earth ions in a noncubic compound. Although determined with a poor accuracy, these negative two-ion quadrupolar coefficients are of the same order of magnitude as those determined in some cubic Pr compounds, as in PrMg<sub>2</sub> (Ref. 34) or PrPb<sub>3</sub>.<sup>35</sup>

### ACKNOWLEDGMENTS

We are grateful to Dr. J. Rouchy for the elastic constant measurements. We warmly thank Dr. R. Lemaire for encouragements and fruitful discussions and Dr. I. Campbell for critical reading of the manuscript. One of us (V.M.T.S.B.) received financial support from the CNPq [Conselho Nacional de Desenvolvimento Científico e Tecnológico (Brazil)], which is gratefully acknowledged.

\*Present address: Instituto de Física, Universidade Federal do Rio de Janeiro, 21944 Rio de Janeiro, Brazil.

<sup>1</sup>M. Giraud, P. Morin, and D. Schmitt, *J. Magn. Magn. Mat.* **52**, 41 (1985).

<sup>2</sup>J. Kötztler, *Z. Phys. B* **55**, 119 (1984).

<sup>3</sup>G. Creuzet et I. A. Campbell, *Phys. Rev. B* **23**, 3375 (1981).

<sup>4</sup>G. Creuzet et I. A. Campbell, *J. Phys. (Paris)* **43**, 809 (1982).

<sup>5</sup>D. Gignoux, A. Nait Sada, and R. Perrier de la Bâthie, *J. Phys. (Paris) Colloq.* **40**, C5-188 (1979).

<sup>6</sup>G. Aubert, D. Gignoux, B. Hennion, B. Michelutti, and A. Nait Saada, *Solid State Commun.* **37**, 741 (1981).

<sup>7</sup>D. Gignoux, B. Hennion, and A. Nait Saada, *Crystalline Electric Field Effects in f-electron Systems* (Plenum, New York, 1982), p. 485.

<sup>8</sup>J. Hog and P. Touborg, *Phys. Rev. B* **11**, 520 (1975).

<sup>9</sup>P. Pureur, G. Creuzet, and A. Fert, *J. Magn. Magn. Mat.* **53**, 121 (1985).

<sup>10</sup>P. Pureur, G. Creuzet, and A. Fert, *J. Magn. Magn. Mat.* **60**, 161 (1986).

<sup>11</sup>P. Hendy, K. M. Al-Rawi, E. W. Lee, and D. Melville, *J. Phys. F* **9**, 2121 (1979).

<sup>12</sup>R. S. Craig, S. G. Sankar, N. Marzouk, V. U. S. Rao, W. E. Wallace, and E. Segal, *J. Phys. Chem. Solids* **33**, 2267 (1972).

<sup>13</sup>K. Andreas and S. Darack, *Physica (Utrecht)* **86**, 1071 (1977).

<sup>14</sup>K. Andreas, S. Darack, and H. R. Ott, *Phys. Rev. B* **19**, 5475 (1979).

<sup>15</sup>P. A. Alekseev, A. Andreeff, H. Griessmann, L. P. Kaun, B.

Lippold, W. Matz, I. P. Sadikov, O. D. Chistyakov, I. A. Markova, and E. M. Savitskii, *Phys. Status Solidi B* **97**, 87 (1980).

<sup>16</sup>H. R. Ott, K. Andreas, E. Bucher, and J. P. Maita, *Solid State Commun.* **18**, 1303 (1976).

<sup>17</sup>B. Lüthi and H. R. Ott, *Solid State Commun.* **33**, 717 (1980).

<sup>18</sup>K. H. J. Stevens, *Proc. Phys. Soc. London, Sect. A* **65**, 209 (1952).

<sup>19</sup>M. T. Hutchings, *Solid State Phys.* **16**, 227 (1964).

<sup>20</sup>P. Morin and D. Schmitt, *Phys. Rev. B* **27**, 4412 (1983).

<sup>21</sup>D. Givord, P. Morin, and D. Schmitt, *J. Magn. Magn. Mat.* **40**, 121 (1983).

<sup>22</sup>E. de Lacheisserie, *Ann. Phys. (N.Y.)* **5**, 267 (1970). Note that the expressions of this reference have been adapted to the quantum treatment used here.

<sup>23</sup>P. Morin, J. Rouchy, and D. Schmitt (unpublished).

<sup>24</sup>Y. L. Wang, *Phys. Lett. A* **35**, 383 (1971).

<sup>25</sup>P. Morin, D. Schmitt, and E. de Lacheisserie, *Phys. Rev. B* **21**, 1742 (1980).

<sup>26</sup>P. Morin and D. Schmitt, *Phys. Rev. B* **23**, 5936 (1981).

<sup>27</sup>V. M. T. S. Barthem and D. Gignoux (unpublished).

<sup>28</sup>V. U. S. Rao and W. E. Wallace, *Phys. Rev. B* **2**, 4613 (1970).

<sup>29</sup>E. P. Wohlfarth and P. Rhodes, *Philos. Mag.* **7**, 1817 (1962);

D. Givord, J. Laforest, and R. Lemaire, *J. Appl. Phys.* **50**,

7489 (1979).

<sup>30</sup>J. Rouchy (private communication).

<sup>31</sup>B. Butler, D. Givord, F. Givord, and S. B. Palmer, *J. Phys. C*

- 13, L743 (1980).
- <sup>32</sup>D. Gignoux, D. Givord, and A. Del Moral, *Solid State Commun.* **19**, 891 (1976).
- <sup>33</sup>A. Naït, Saada, Thesis, University of Grenoble, 1980.
- <sup>34</sup>A. Loidl, K. Knorr, M. Müllner, and K. H. J. Buschow, *J. Appl. Phys.* **52**, 1433 (1981).
- <sup>35</sup>P. Morin, D. Schmitt, and E. de Lacheisserie, *J. Magn. Magn. Mat.* **30**, 257 (1982).